

RESEARCH

Open Access



Leveraging AAV1-Rac1T17N to prevent experimental proliferative vitreoretinopathy

Duo Li^{1,2†}, Minli Linghu^{1†}, Jisen Tang^{1,2†}, Gukun Yang^{1,2}, Chuanwu Li¹, Hang Yao¹, Hetian Lei^{1*}, Yikeng Huang^{3*} and Xionggao Huang^{1,2*}

Abstract

Background Platelet-derived growth factor receptor β (PDGFR β) is the principal PDGFR isoform in retinal pigment epithelial (RPE) cells from the epiretinal membranes of patients with proliferative vitreoretinopathy (PVR). Ras-related C3 Botulinum toxin substrate 1 (Rac1), a member of the Rho family, is a crucial factor in the cell migration and contraction processes that are inherent to the pathogenesis of PVR. The mutants Rac1T17N and Rac1Q61L can block and promote Rac1 activation, respectively. The major objective of this research was to ascertain whether PDGFR β mediates vitreous-induced Rac1 activation and whether Rac1T17N could be leveraged for the prevention of PVR pathogenesis in a rabbit model.

Methods A pull-down assay was used to examine GTP Rac1 levels, which are indicative of Rac1 activation, and western blotting was used to assess cellular protein expression. A CCK8 assay, a wound healing assay, a transwell invasion assay and a collagen contraction assay were employed to analyze cell proliferation, migration, invasion and contraction capacity, respectively. A PVR model was created by injecting platelet-rich plasma and human retinal pigment epithelial cells (ARPE-19) into the vitreous cavities of rabbits, and this model was used to evaluate the severity of PVR impacted by intravitreally injected ARPE-19 cells transduced with adeno-associated virus (AAV)1-Rac1T17N or Rac1Q61L. PVR grade was evaluated by a double-blinded investigator according to the Fastenberg classification; in addition, ultrasound and histological analyses were performed to assess PVR severity.

Results Vitreous-induced GTP Rac1 is mediated by PDGFR β . There was a significant decrease in vitreous-induced GTP Rac1 in ARPE-19 cells transduced with AAV1-Rac1T17N compared with those transduced with AAV1-GFP. In addition, the suppression of GTP Rac1 production in human RPE cells by transduction with AAV1-Rac1T17N inhibited vitreous-induced proliferation, migration, invasion, and contractility. Importantly, the results of the animal experiments indicated that although there was a significant increase in PVR potential in rabbits intravitreally injected with ARPE-19 cells infected with AAV1-Rac1Q61L, there was a significant decrease in PVR potential in rabbits intravitreally injected with ARPE-19 cells infected with AAV1-Rac1T17N ($P < 0.01$).

Conclusions AAV1-Rac1T17N has great potential for PVR therapy.

Keywords PDGFR β , Rac1T17N, RPE cells, Vitreous, Contraction, PVR

[†]Duo Li, Minli Linghu, and Jisen Tang have contributed equally to this work.

*Correspondence:

Hetian Lei

Leihetian18@hotmail.com

Yikeng Huang

chaos_k@sjtu.edu.cn

Xionggao Huang

hxg_eye@163.com

Full list of author information is available at the end of the article



Introduction

Proliferative vitreoretinopathy (PVR) is a severe complication of retinal detachment surgery or ocular trauma and is also a major factor of retinal detachment repair failure that can lead to vision loss or severe blindness [1–3]. Five to ten percent of patients with retinal detachment develop PVR, and surgical treatment is currently the mainstay, though the repair is prone to relapse after surgery [4, 5]. Although a great deal of research has been conducted to explore the clinical and basic aspects of this condition, the exact mechanism is still not well understood. Some anti-inflammatory and anti-proliferative activity agents such as corticosteroids and methotrexate have been used in clinical trials, but there are limitations to their efficacy and consistency of data [6]. Therefore, it is crucial to further understand its molecular mechanisms to identify more effective therapeutic targets.

In recent years, platelet-derived growth factor receptor (PDGFR) has attracted considerable attention. Researchers have reported that interfering with PDGFR α in retinal pigment epithelial (RPE) cells effectively inhibits the progression of the proliferative membrane in PVR [7]. PDGFR β inhibition largely suppresses vitreous-induced cellular responses associated with PVR pathogenesis [8]. Recently, our group showed that the lncRNA MALAT1 mediates epithelial–mesenchymal transition (EMT) in RPE cells through PDGFR/AKT signaling [9]. Because PDGFR promotes cellular EMT and thereby determines the pathogenesis of PVR, further studies are needed to elucidate the molecular regulatory mechanisms downstream of PDGFR.

Ras-related C3 botulinum toxin substrate (Rac)1 is a typical member of the Rho family, and as a molecular signaling switch, Rac1 regulates numerous important cellular functions [10–12]. In particular, as a cytoskeletal protein, Rac1 has been implicated in regulating cytoskeletal reorganization, cell adhesion, cell morphology and cell motility [13]. Rac1 shifts from a GDP-bound inactive state to a GTP-bound active state in the presence of guanine nucleotide exchange factor (GEF), which triggers a downstream signaling cascade response [14, 15]. Our previous study revealed that Rac1 was activated in vitreous-transformed RPE cells [16]. Rac1 GTPase regulates cytoskeletal reorganization of the RPE through the activation of LIM kinase 1 (LIMK1) to phosphorylate cofilin [16, 17]. Moreover, the Rac1 inhibitor NSC23766 can inhibit the vitreous-induced migration and invasion ability of RPE cells [17]. Therefore, Rac1 is a key pathogenic molecule in the pathogenesis of PVR, and targeting Rac1 is expected to be a new therapeutic approach for PVR.

Most recently, several studies have proposed that PDGFs/PDGFRs potentially participate in the regulation of Rac1 to play important roles in tumor cells [18–20].

However, the mechanism by which vitreous-induced PDGFR regulates GTP Rac1 in RPE cells has not yet been elucidated. The effects of GTP Rac1 levels on the development of PVR in vitro and in vivo remain to be investigated.

The aim here is to investigate whether PDGFR β has a regulatory role for GTP Rac1, to detect the effects of changes in GTP Rac1 activity at the cellular level on its biological function, and to probe the effect of this signaling axis on the severity of PVR. Based on in vitro experimental evidence, our study revealed that PDGFR β mediates vitreous-induced Rac1 activation and that GTP-Rac1 promotes the proliferation, migration, invasion, and contractile functions of RPE cells. Furthermore, the in vivo results demonstrated that experimental PVR could be prevented by the use of AAV1-Rac1T17N. This study provides new perspectives for the treatment of PVR.

Materials and methods

Major reagents

An antibody against Rac1 (1:1000) was procured from Millipore (17–283, Billerica, MA, USA); antibodies against platelet-derived growth factor receptor (PDGFR) β (#3169, 1:1000), β -actin (#4970, 1:4000), α -smooth muscle actin (SMA) (#19245, 1:1000), and p38 MAPK (#8690, 1:1000) were obtained from Cell Signaling Technology (Danvers, MA); a Rac activity assay kit was obtained from Millipore (17–283, Billerica, MA, USA); antibodies against JNK (#66210, 1:10000), phospho-JNK (#80024, 1:2000) were purchased from Proteintech (Wuhan, China); and antibodies against phospho-p38 (AB195049, 1:1000), ERK (AB184699, 1:10000), and phospho-ERK (AB278538, 1:5000) were obtained from Abcam (Cambridge, UK). Horseradish peroxidase-conjugated anti-mouse/rabbit immunoglobulin G antibodies were acquired from Beyotime (A0216/A0208; Shanghai, China). Fluorescein isothiocyanate (FITC)-labeled phalloidin was obtained from Sigma (P5282, Sigma–Aldrich, St. Louis, MO, USA).

Cell culture and vitreous treatment

A spontaneously arising human retinal pigment epithelial cell line (ARPE-19 cells, RRID: CVCL-0145) was purchased from the BeNa Culture Collection (China). The cells were cultured in DMEM/F12 medium (Gibco, Life Technologies) supplemented with 10% fetal bovine serum (Gibco, Life Technologies) and 1% penicillin/streptomycin (Gibco, Life Technologies) at 37 °C in a humidified tissue culture chamber containing 5% carbon dioxide. Cells from passages 3 to 5 were used for further experiments.

Frozen rabbit eyeballs were used to generate rabbit vitreous (RV), which was carefully separated from the retina in the frozen state, collected after completely dissolving and then centrifuged at $13,000\times g$ for 5 min at 4 °C. A volume fraction of 25% RV in DMEM/F12 medium was used as described previously [21].

Immunofluorescence

Cells were plated onto sterilized slides at 2×10^4 cells/slide and incubated in normal medium or RV for 24 h. After being washed 3 times with precooled PBS, the cells were first treated with 4% paraformaldehyde for 10 min. Next, the cells were gently washed with PBS 3 times, each time for 10 min. Then, the cells were stained with fluorescein isothiocyanate (FITC)-labeled phalloidin (5 µg/ml, P5282, Sigma–Aldrich, St. Louis, MO, USA) at 37 °C for 1 h and photographed under a confocal microscope (FV1000, Olympus) [16].

Western blot

A total of 2×10^5 cells per well were dispensed evenly into 24-well plates and were allowed to attach to the walls and grow to 90% confluence. The cells were deprived of serum for the duration of the night before being treated as needed. Protein extraction and quantification were accomplished following adequate cell lysis on ice with RIPA lysis buffer. Multiple target proteins were then isolated and then transferred to PVDF membranes. The samples were subsequently blocked in TBST containing 5% nonfat milk powder for 1 h on a shaker and then cultured with primary antibodies including anti-Rac1 (1:1000), anti-β-actin (1:4000), anti-PDGFRβ (1:1000), and anti-α-SMA (1:1000) at 4 °C overnight. The antibody-bound membranes were rinsed thoroughly on a shaker with TBST for 5 min each time for a total of 3 washes and subsequently exposed to a horseradish peroxidase-labeled anti-mouse/rabbit IgG secondary antibody for 1 h at room temperature. After secondary antibody incubation, the sections were thoroughly rinsed as previously described. Finally, the antibody-bound membranes were developed with an ECL luminescence kit [16]. We use Image J software to analyze the grayscale values of the bands obtained, convert the images captured by the fully automatic chemiluminescence image analyzer into 8-bit grayscale images, and use a rectangle tool to select all the bands for analysis to obtain peak maps. The Area value obtained for each peak is the quantized value of each band.

Rac1 activity assay

When the cells adhered to the plate walls and reached approximately 90% confluence, they were deprived of serum overnight and subsequently exposed to RV for 3 h. After the medium was removed, the cells were rinsed twice with ice-cold TBST and lysed in ice-cold 1X Mg²⁺ lysis buffer. Subsequently, the lysates were harvested in microfuge tubes on ice, and 10 µl of Rac1/cdc42 assay reagent (PAK-1 PBD, agarose) was pipetted per 0.5 ml of cell lysate. The samples were gently rocked at 4 °C for 1 h, after which the agarose beads were pelleted by centrifugation at $13,000\times g$ for 10 s and were then resuspended in 2X Laemmli sample buffer. After denaturation by boiling for 5 min, the samples with the GTP-conjugated form of Rac1 were subjected to western blot analysis. Notably, equivalent amounts of untreated cell lysates were exposed to GTPγS or GDP as positive or negative controls [16, 17].

Cell proliferation assay

ARPE-19 cells were inoculated in 96-well plates at 2,000 cells per well. The cells were allowed to adhere sufficiently to the plate walls, after which the cells were incubated with serum overnight. The cells were then incubated with RV in triplicate for 48 h. Next, 10 µl of CCK8 reagent was loaded into each well, and the plates were incubated in a thermostatic incubator for 2 h, after which the absorbances at 450 nm were determined.

Cell migration assay

ARPE-19 cells were grown in 12-well plates (2×10^5 cells/well) to 90% incorporation and then cultured overnight in the absence of serum. Next, the cells were gently rinsed with PBS to remove cell fragments after the cell monolayer was scratched and then treated with RV or cultured normally. Photographs were recorded at 0, 24 and 36 h after the scratches were created. The area of the scratches at 0, 24 and 36 h was evaluated in pixels using Image J software, and the ratio of the scratch area at 24 h and 36 h to the initial scratch area was calculated and then statistically analyzed.

Transwell assay

Transwell chambers (3422, Corning, USA) were plated at a 1:8 ratio of Matrigel (356234, Corning, USA) to serum-free culture solution. Cells in serum-free DMEM/F12 were subsequently inoculated into chambers that had already been processed at approximately 5×10^4 cells per well. After 3 h, the medium in the lower chamber was replaced with either normal medium or RV for 24 h of incubation. After invading cells were fixed for 20 min with 4% paraformaldehyde, crystal violet (0.1%) staining

was performed for 10 min. A random selection of five visual fields was photographed, and the number of invasive cells was counted.

Contraction assay

Trypsin-digested RPE cells were resuspended in neutralized collagen I solution (1.5 mg/ml) (5074, Sigma–Aldrich, St. Louis, MO, USA), and the cell density was adjusted to approximately 1×10^6 cells/ml. The mixture was subsequently transferred to wells in a 24-well plate that had been incubated overnight with 5 mg/ml BSA (0.3 ml mixture/well) in advance. The plate was subsequently incubated at 37 °C for 90 min for collagen solidification, and normal culture medium or RV was subsequently added to the wells. After 24 h and 48 h, the gels were photographed, and the gel diameter was measured using Image J software. The gel area was calculated using the formula πr^2 , where r is the gel radius [16].

Experimental PVR

Experimental PVR was established in pigmented rabbits' left eyes by the injection of 0.1 ml of perfluoropropane (C3F8) 4 mm behind the corneal limbus into the vitreous cavity. All the rabbits were injected with both 0.1 ml of platelet-rich plasma (PRP) and 0.1 ml of DMEM/F12 containing 2.5×10^5 ARPE-19 cells 1 week later. In addition, 10 μ l of AAV1-Rac1-Q61L, -T17N, or -GFP was also intravitreally injected weekly. The fundus of each eye was examined with indirect funduscopy on days 1, 3, 5, 7, 14, 21, and 28, and levofloxacin ophthalmic solution (0.5%, Santen Pharmaceutical Co., Ltd.) was dropped on the eye 3 times daily 3 days before and 3 days after the virus injection [22]. B-ultrasound scans (SW2100, SUOER) was performed at 1, 2, and 4 weeks after injection, and PVR stages were graded from 0 to 5 according to the Fastenberg classification [23]. On Day 28, the rabbits were sacrificed, and the eyes were removed for subsequent experiments. All procedures were performed under aseptic conditions and approved by the ethics committee of the First Affiliated Hospital of Hainan Medical University.

Histological evaluation of retinas

Experimental rabbit eyeballs were fixed and then subjected to paraffin-embedded sectioning for pathological analysis. Briefly, the permeabilized 5 μ m longitudinal sections were immersed in hematoxylin to stain the cell nuclei for 5 min, removed, rinsed under running water for 1 min until the color became violet, and then placed in 1% hydrochloric acid alcohol for 2 s to differentiate the color. Then, the samples were rinsed under running water for 1 min and stained with eosin for 2 min. Finally, gradient alcohol stepwise dehydration was performed, followed by a neutral gum sealing treatment. These sections were observed and recorded under a light microscope.

Statistical analysis

GraphPad Prism 8 was performed for statistical analyses. One-way analysis of variance (ANOVA) was used for statistical analysis of data from three independent experiments. $p < 0.05$ was considered to indicate a significant difference.

Results

Phosphorylation of PDGFR β is significantly increased and knockdown of PDGFR β inhibits Rac1 GTP activity in rabbit vitreous-transformed ARPE-19 cells

Total PDGFR β protein expression in ARPE-19 cells was not significantly altered by stimulation of the rabbit vitreous, in contrast to phosphorylated PDGFR β receptors, which were significantly increased after vitreous stimulation (Fig. 1E, H, I). To confirm the relationship between PDGFR β and Rac1, we generated PDGFR β -overexpressing ARPE β cells and PDGFR β -nonexpressing ARPE-KD cells (Fig. 1A–D). Then, 25% RV was used to induce PDGFR β expression and activation (cells were cultured in DMEM/F12 as control), and changes in Rac1 expression or activity were detected by culturing the cells separately. The findings demonstrated that Rac1 activity was considerably increased in ARPE β cells but markedly reduced in ARPE-KD cells compared with ARPE-19 cells with 25% RV-stimulated cells (Fig. 1E, F). However, there was no significant change in total Rac1 protein in either the control or the 25% RV experimental groups (Fig. 1E,

(See figure on next page.)

Fig. 1 Effect of PDGFR β expression on Rac1 protein expression levels. **A** Diagram of PDGFR β -sgRNA from exon 3. Identified by red arrows are expected cleavage sites. In the sequence of three nucleotides colored blue, there are protospacer adjacent motifs (PAM). **B** Sequencing results after amplification of the DNA fragment around the PAM sequence. Identified by red arrows are expected cleavage sites, and the removal of two nucleotides is indicated by a red star. **C** Expression of PDGFR β was examined by Western blot analysis. ARPE β : PDGFR β overexpression cell line; ARPE-KD: PDGFR β knockdown cell line. **D** Quantification of the PDGFR β expression (normalized to β -actin). The mean \pm SD of three independent experiments is presented. **E, F** Enhanced GTP Rac1 in the ARPE β group and reduced GTP Rac1 in the ARPE-KD group induced by 25%RV. Quantification of the GTP Rac1 expression (normalized to β -actin). **E, G** No significant trend was observed for total Rac1 protein. Quantification of the total Rac1 expression (normalized to β -actin). **E, H, I** Expression of PDGFR β and p-PDGFR β were examined by Western blot analysis. Quantification of PDGFR β and p-PDGFR β expression (normalized to β -actin)

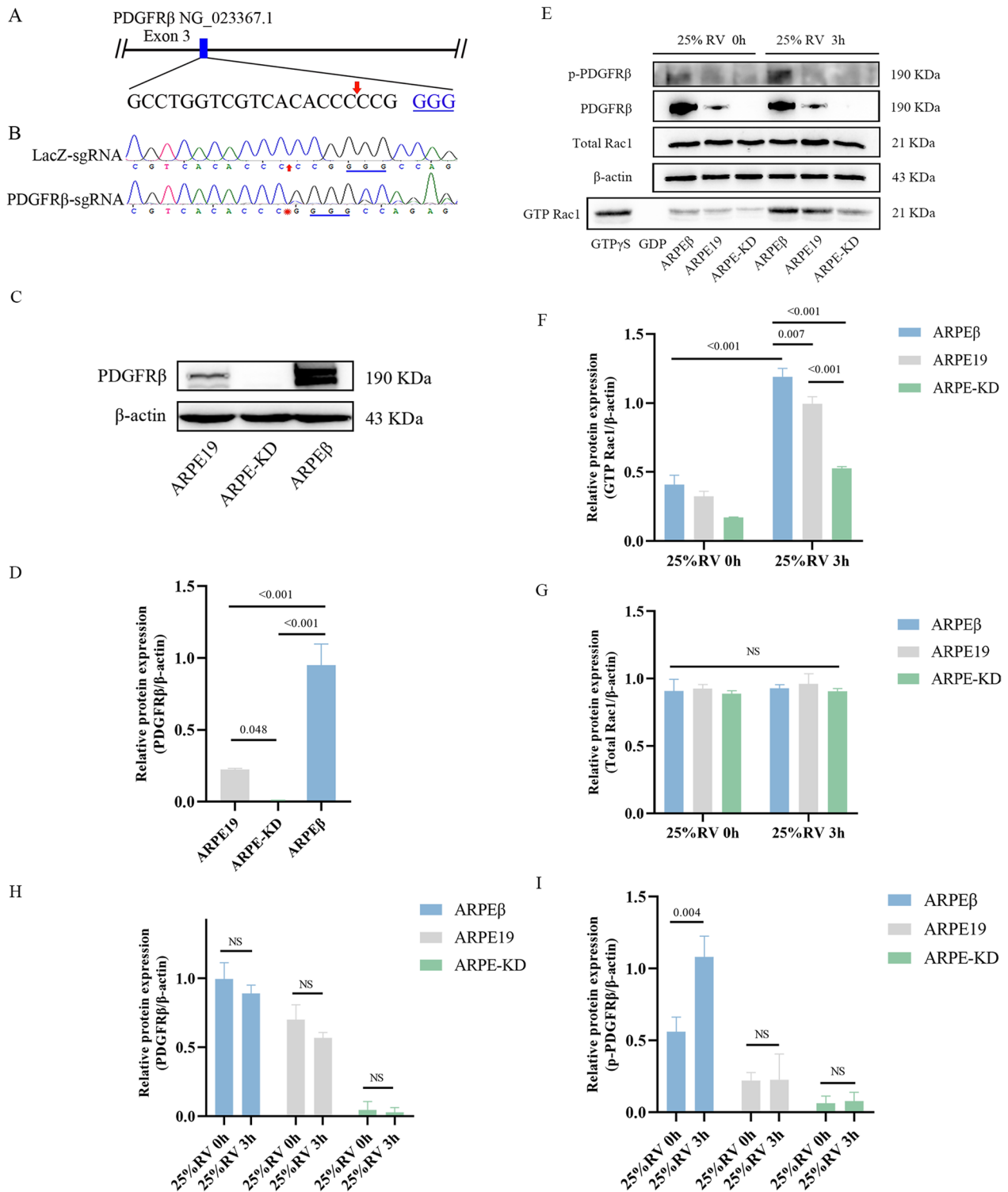


Fig. 1 (See legend on previous page.)

G). These findings indicate that PDGFRβ is involved in regulating Rac1 GTP activity in 25%RV-stimulated ARPE-19 cells.

Rac1 activation is attenuated in RPE cells expressing the dominant-negative mutant Rac1 T17N
Because Rac1 is crucial in the pathogenesis of PVR, we

managed to find a novel approach to restrain Rac1 activation. For this purpose, we infected ARPE-19 cells with rAAV expressing a dominant-negative mutant, Rac1-T17N; ARPE-19 cells infected with rAAVs expressing a dominant-positive mutant, Rac1-Q61L, or GFP were used as controls. Our previous results showed that the GTP Rac1 levels peaked at 3 h of the vitreous stimulation, so we chose the 3-h time point for the follow-up study [24]. These cells were exposed to RV for 3 h, and their lysates were subjected to a Rac1 GTP pull-down assay. The findings demonstrated that the T17N mutation significantly suppressed Rac1 GTP activity (Fig. 2A, B). In contrast, total Rac1 levels did not change (Fig. 2A, C). Because PDGFR β is an integral contributor to experimental PVR, we examined the levels of PDGFR β in

treated cells. The data revealed that the level of phosphorylated PDGFR β was significantly affected by the level of the GTP Rac1 (Fig. 2D, E).

Rac1T17N reverses vitreous-induced morphological changes and cytoskeletal reorganization in RPE cells

To investigate the impact of the Rac1 mutants Q61L and T17N on cell morphological changes and skeletal reorganization, we infected ARPE-19 cells with rAAV1-Q61L-GFP and rAAV1-T17N-GFP, respectively. F-actin in these infected cells was then labeled with a FITC-labelled phalloidin, and these cells were subjected to phase contrast microscopy and laser confocal microscopy. As shown in Fig. 3A–D, in normal medium, the four cell types grew in clusters with extensive contact

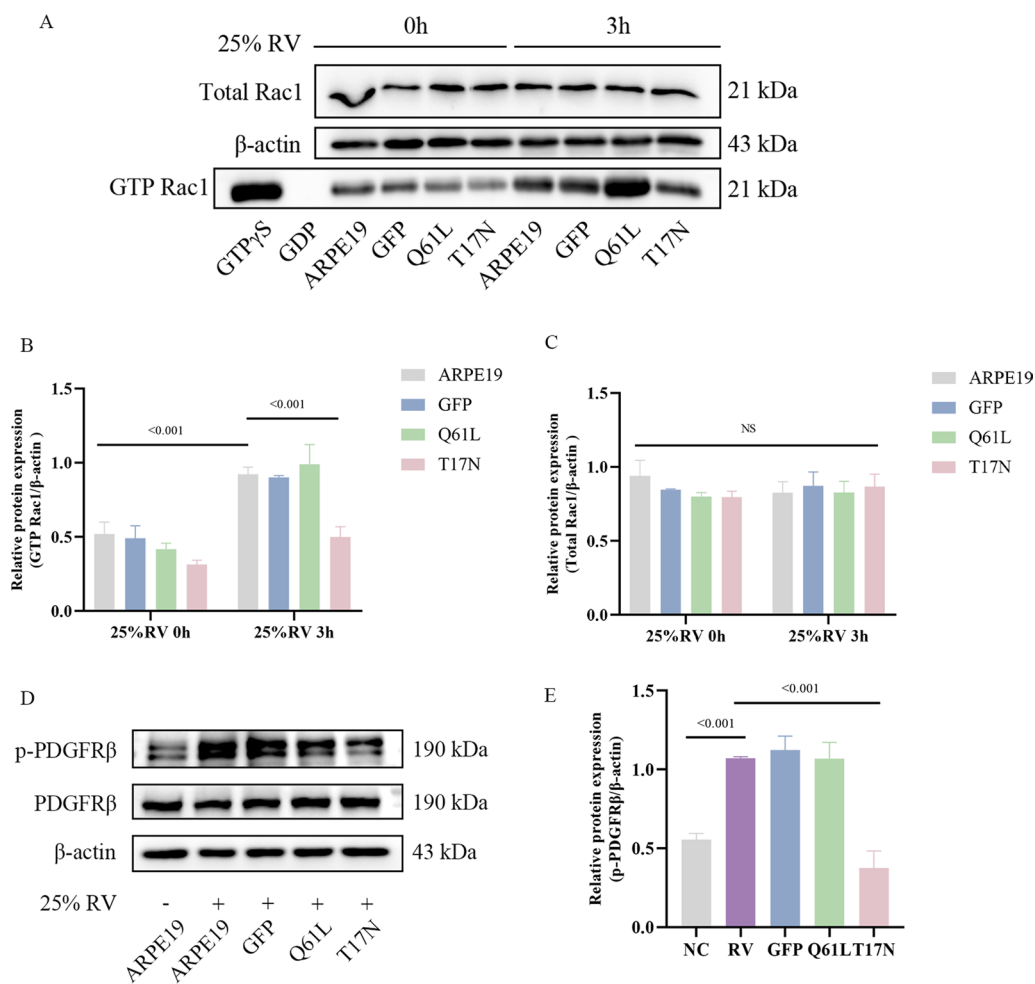


Fig. 2 Rac1T17N and Rac1Q61L decreased and increased vitreous-induced Rac1 activation, respectively. **A** Expression of GTP Rac1 and total Rac1 in ARPE-19 cells infected by AAV1-Rac1-GFP, -Q61L, or -T17N was examined by Western blot analysis. **B, C** Quantification of the relative protein expression (normalized to β-actin). The mean ± Standard deviation (SD) of three independent experiments is shown. **D** Expression of PDGFR β and p-PDGFR β in ARPE-19 cells infected by AAV1-Rac1-GFP, -Q61L, or -T17N was examined by Western blot analysis. **E** Quantification of the relative protein expression (normalized to β-actin). The mean ± Standard deviation (SD) of three independent experiments is shown

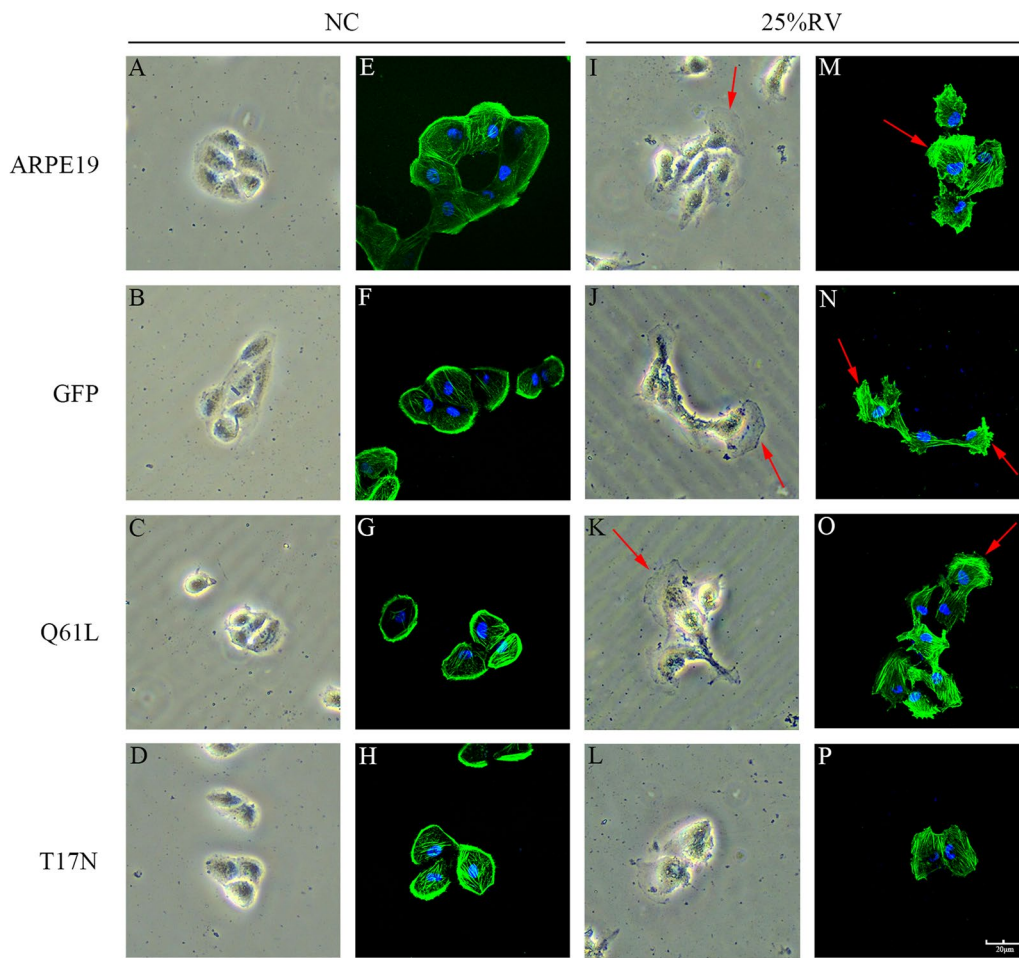


Fig. 3 Rac1T17N and RacQ61L respectively regulated vitreous-induced morphological changes and cytoskeleton reorganization. **A–D** Impact of Rac1T17N and Q61L on morphology of normal cultured ARPE-19 cells. $\times 100$. **E–H** Impact of Rac1T17N and Q61L on F-actin distribution in ARPE-19 cells cultured in normal condition. Cells were stained with FITC-labeled phalloidin. $\times 600$. **I–L** Impact of Rac1T17N and Q61L on morphology of ARPE-19 cells treated with RV. **I–K** ARPE-19 cells expressing GFP or Rac1 Q61L cells showed a spindle or fan-shaped cell morphology (The red arrow points to the cell morphology changes) when treated with RV. **L** ARPE-19 cells expressing Rac1 T17N remained an epithelial morphology when treated with RV. $\times 100$. **M–O** The cytoskeleton of ARPE-19 cells expressing GFP or Rac1 Q61L cells and being treated with RV reorganized to form protrusions, mainly on one side of the cell, in a flattened pseudopod-like rearrangement (The red arrow points to the flattened pseudopodium formed by the reorganization of cytoskeleton). **P** The F-actin of ARPE-19 cells expressing Rac1 T17N and being treated with RV was mainly localized in the pericellular region. $\times 600$

among the cells and remained in a resting flat state, whereas in RV-treated ARPE-19 and Q61L-infected cells, their morphology shifted to a spindle or fan-shaped cellular morphology (Fig. 3I–K). Notably, the rAAV-T17N-infected cells remained flattened (Fig. 3L).

Immunofluorescence analysis revealed that F-actin was mainly localized around the cells in the normal medium culture group (Fig. 3E–H), whereas in the ARPE-19 cells treated with RV, the rAAV1-GFP- or Q61L-infected cells underwent cytoskeletal rearrangement, with actin rearranging and forming protrusions that formed flattened pseudopods predominantly on one side of the cells (Fig. 3M–O). In contrast, F-actin was redistributed

around the cells expressing T17N (Fig. 3P). These findings indicate that the vitreous humor induces GTP Rac1 activation, which is required for vitreous-stimulated cell morphological changes and cytoskeletal rearrangement.

Rac1T17N inhibits vitreous-induced migration, proliferation and invasion of RPE cells

We next assessed whether enhancement or attenuation of Rac1 activity with its mutants would alter the migration, proliferation, and invasion capacities of human RPE cells. ARPE-19 cells infected with AAV1-Rac1Q61L, T17N, or GFP were treated with RV and then subjected to a cell migration assay, a CCK8 assay for proliferation,

and an invasion transwell assay. The results revealed that the cells in the Rac1Q61L group migrated fastest and had the highest migration rate at 36 h among the five groups, whereas the cells in the Rac1T17N group presented decreased migratory ability (Fig. 4A, B).

Similar results were obtained with the CCK8 and transwell assays. ARPE-19 cells expressing Rac1Q61L presented the highest OD at 450 nm, which is indicative of their proliferation potential, and the OD peaked at 48 h after RV stimulation (Fig. 4C). In the cell invasion assay, the number of invasive cells with both Rac1Q61L and GFP considerably increased compared with those without RV stimulation. In addition, the number of ARPE-19 cells with Rac1T17N treated with RV was notably reduced than that of the control group with RV treatment (Fig. 4D–I).

Rac1T17N hampers vitreous-induced cell contraction

The contractile force of epiretinal membranes leads to retinal detachment in the pathogenesis of PVR. Next, a collagen contraction assay was performed to assess whether Rac1T17N could prevent vitreous-induced cell contraction. As shown in Fig. 5, compared with that of ARPE-19 cells in normal culture, the vitreous contractility of ARPE-19 cells transduced with AAV1-GFP or Rac1Q61L was greater; however, this enhancement was diminished in ARPE-19 cells infected with AAV1-Rac1T17N (Fig. 5B, C). Furthermore, this Rac1 mutation also blocked the vitreous-induced increase in α -SMA (Fig. 5A, D).

Cellular responses intrinsic to PVR are mediated by Rac1 signaling through the MAPK pathway

Although the role of Rac1 in the MAPK pathway has been reported in several other studies [25–27], it is not clear whether Rac1 mediates functional changes in the RPE via the MAPK pathway. To investigate the effects of vitreous and Rac1 activity levels on the MAPK signaling pathway, we examined changes in ERK, p38, and JNK expression. As shown in Fig. 6A, B, phosphorylated ERK expression showed a high degree of concordance with Rac1 activity levels, with vitreous-stimulated ERK phosphorylation levels significantly higher than those of the controls, and Rac1 activity levels were increased by transfection with AAV1-Q61L, which further increased, whereas T17N reversed this trend. In addition, we analyzed other members of the MAPK pathway, including p38 and JNK, and as shown in the results, both phosphorylated p38 and phosphorylated JNK were significantly altered by the transfection of different adeno-associated viruses to control GTP Rac1 levels (Fig. 6C–F). These results indicate that the GTP Rac1 may function through the MAPK signaling pathway.

Rac1T17N suppresses experimental PVR whereas Rac1Q61L increases PVR potential in a rabbit model

We next attempted to assess the importance of Rac1 activity in promoting PVR in an experimental rabbit model. Therefore, we intravitreally injected rabbits with platelet-containing plasma and ARPE-19 cells transduced with rAAV1 expressing GFP, Rac1Q61L or Rac1T17N. The severity of PVR was significantly exacerbated when cells expressing the Rac1Q61L virus were injected (Fig. 7A). Specifically, 90% of rabbits progressed to grade 3 or higher retinal detachment at 28 days, whereas only 20% of rabbits injected with cells expressing Rac1T17N developed grade 3 or higher retinal detachment.

To examine the degree of vitreous turbidity and peripheral vitreoretinal lesions, we performed B-ultrasound scans on all rabbits. In the normal group, there was no significant abnormal echogenicity in the vitreous cavity (Fig. 7B), whereas in the group that was infused with cells expressing Rac1Q61L, striated echogenicity and a band of echogenicity connected to part of the spherical wall were observed. In addition, vitreous opacification and retinal detachment occurred in the rabbit model (Fig. 7C, D). Importantly, in the group treated with cells expressing Rac1T17N, no markedly abnormal echogenicity was observed in the vitreous (Fig. 7E).

Pathology with HE staining revealed a clear structure of the whole layer of the normal rabbit retina, and the cells of the ganglion cell layer and the inner and outer nuclear layers were neatly arranged (Fig. 7F). However, in the rabbits injected with cells expressing GFP, there was complete detachment of the retinal neuroepithelium from the retinal pigment epithelium (Fig. 7G), whereas in the rabbits injected with cells expressing Q61L, we observed retinal detachment from the neuroepithelium and choroid; in particular, an edematous ganglion cell layer and loss of photoreceptor cells were observed in this group of rabbits (Fig. 7H). In contrast, in rabbits injected with cells harboring Rac1T17N, the retinal structure was clearer, and the degree of retinal detachment was significantly lower than those in the GFP and Q61L groups (Fig. 7I).

Discussion

The main cell type involved in PVR is RPE cells, as they are major constituents of ERMs [1, 2]. When rhegmatogenous retinal detachment occurs, the blood–retinal barrier is impaired. Consequently, RPE cells migrate from their regular anatomical position into the vitreous cavity through the retinal fissure. With the stimulus of abundant cytokines and growth factors that exit the vitreous space, RPE cells are subjected to epithelial–mesenchymal transition (EMT) and obtain a mesenchymal phenotype, which is associated with increased migration, invasion, and resistance to apoptosis [1–3, 28, 29]. Research has

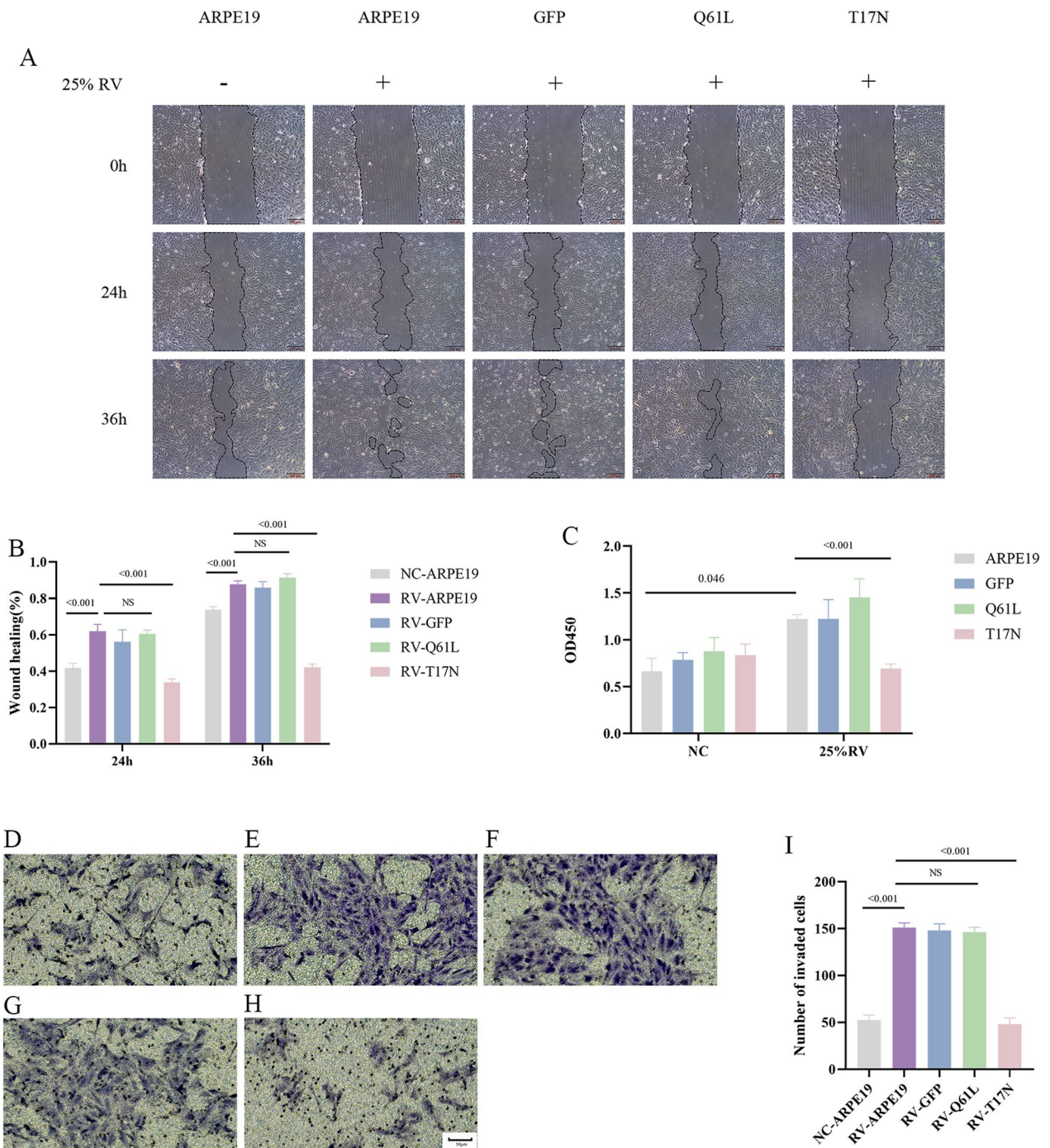


Fig. 4 Rac1T17N and Rac1Q61L diminished and enhanced vitreous-induced cellular responses related to PVR, respectively. **A** Respectively images of wound areas ($\times 100$) are shown. GFP, T17N, and Q61L denote the ARPE-19 cells transduced by AAV1-GFP, Rac1T17N, and Rac1Q61L, respectively. **B** The mean \pm SD of three independent experiments is shown. Data are the percentage of wound size presented. **C** The absorbance value was measured at a wavelength of 450 nm for the cell proliferation capacity. The mean \pm SD of three independent experiments is shown. **D**, **E** Representative images of invaded ARPE-19 cells in the normal culture medium and RV. **F–H** Representative images of invaded ARPE-19 cells transduced by AAV1- GFP, -Rac1Q61L, and Rac1T17N when treated with RV. $\times 200$. **I** The mean \pm SD of five independent experiments from D-H is shown

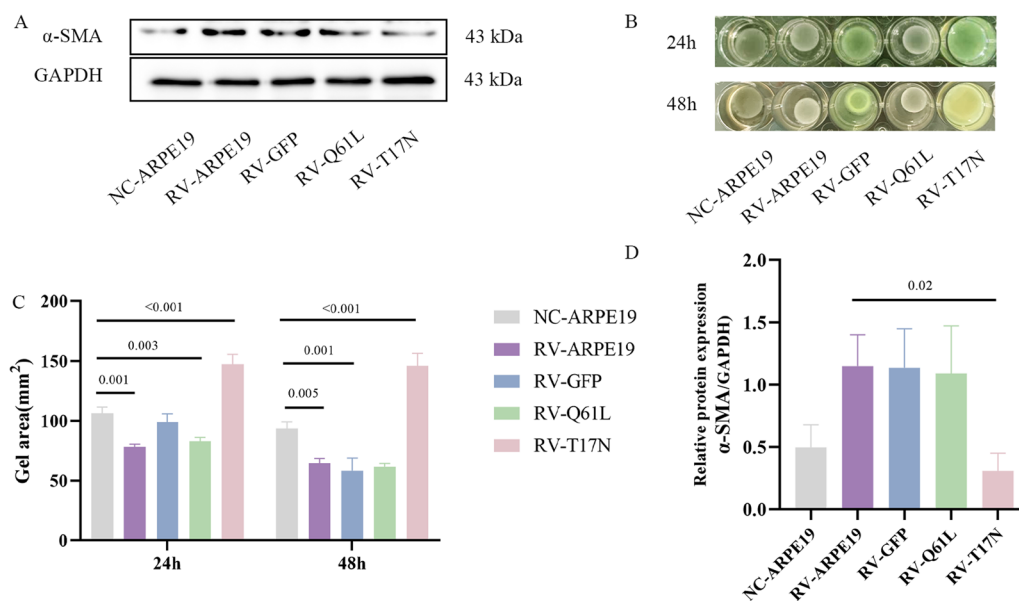


Fig. 5 Rac1T17N and Rac1Q61L suppressed and promoted vitreous-induced contraction of RPE cells, respectively. **A** Rac1Q61L and Rac1T17N enhanced and reduced RV-induced expression of α -SMA in ARPE-19 cells. **B, C** Rac1T17N suppressed RV-stimulated cell contraction. Gels were photographed at 24 h and 48 h after RV stimulation. The mean \pm SD of three independent experiments is shown. **D** Quantification of the relative protein expression (normalized to GAPDH) in western blot; the mean \pm SD of three independent experiments was presented

shown that the non-PDGF (e.g., rabbit vitreous)-stimulated PDGFR pattern plays a crucial role in the pathological basis of PVR [22, 30]. In this work, we used 25% RV as a stimulus for ARPE-19 cells to simulate this pathological process. Although cell/growth factor/vitreous interactions with respect to the pathogenesis of PVR are currently accepted, the finer details of the signaling pathways are not clearly understood. Our study clarified the key issue of whether there is a correlation between vitreous stimulation of PDGFR β and Rac1. We found that the Rac1 activity of cells with high PDGFR β expression was significantly enhanced by 25% RV stimulation, in contrast to the greatly reduced Rac1 activity after PDGFR β expression on the cell membrane was knocked down. Thus, the extent to which PDGFR β is activated in the cell membrane plays a regulatory role in Rac1 activity.

We have shown in this study that the suppression of Rac1 activity using its mutant Rac1T17N suppressed the vitreous-induced migration, invasion, proliferation, and contractility of human RPE cells together with PVR development in an experimental rabbit model established by the intravitreal injection of RPE cells [3].

One of our research goals in this project was to discover therapeutic approaches for PVR development. Rac1 plays an important role in carcinogenesis. For example, Rac1 overexpression and activation have been observed in various malignancies, including gastric, colon and bladder cancers [31–33]. The oncogenic mutant Rac1Q61L along with the negative control

site T17N are notable. Rac1Q61L inhibits the GAP-stimulated hydrolysis of GTP to GDP, which keeps the GTPase in an activated state [12, 34]. Rac1T17N is present in a nucleotide-free or inactive state, which results in competitive binding with the GEF [34]. Inhibition of Rac1 by various methods such as Rac1 conditional knockout, inhibitor NSC23766 has been studied in diseases such as glaucoma and choroidal neovascularization [35, 36]. In the present study, the inhibition of GTP Rac1 by T17N may provide more evidence to study the intrinsic mechanism of Rac1 in retinal diseases.

Due to their stability, efficiency and noncytotoxicity, rAAV-based gene delivery vectors have proven to be reliable and efficacious for numerous clinical gene therapy applications [37, 38]. Their safety and efficacy have been demonstrated in many diseases, including glioblastoma, cardiovascular disease and many eye diseases [38–40]. We leveraged the rAAV system to deliver the Rac1 mutants Q61L and T17N, which positively or negatively regulate Rac1 activity, into ARPE-19 cells, demonstrating that Rac1 is essential for vitreous-induced responses among cells (e.g., migration and contraction) involved in the etiology of PVR. This series of experiments also revealed that AAV1-Rac1T17N has great potential for PVR therapy. Gene therapy has brought hope for curing many diseases, this research not only advances theoretical understanding but also provides practical insights that can be leveraged in real application.

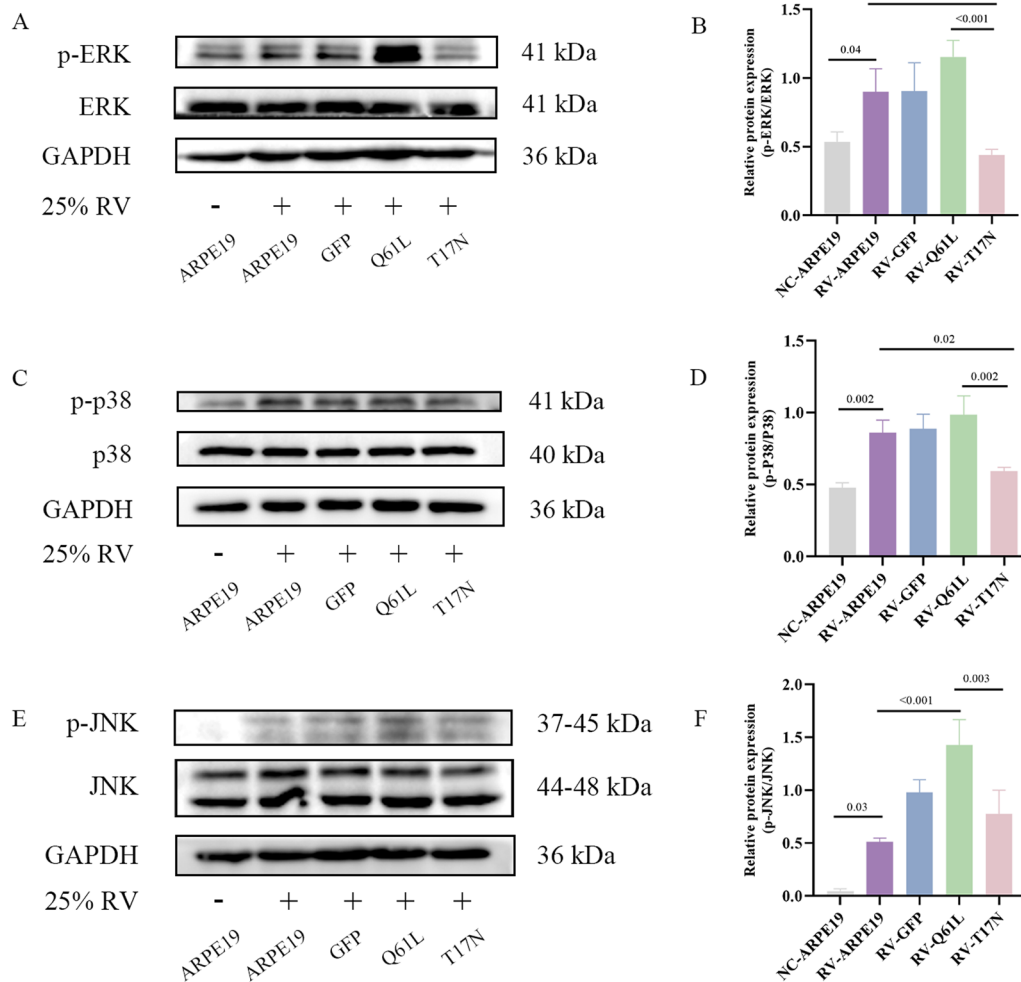


Fig. 6 Rac1T17N and Rac1Q61L decreased and increased vitreous-induced MAPK pathways. **A, B** Expression of ERK and p-ERK in ARPE-19 cells infected by AAV1-Rac1-GFP, -Q61L, or -T17N was examined by western blot analysis. Quantification of the relative protein expression (normalized to ERK). The mean \pm Standard deviation (SD) of three independent experiments is shown. **C, D** Expression of p38 and p-p38 in ARPE-19 cells infected by AAV1-Rac1-GFP, -Q61L, or -T17N was examined by western blot analysis. Quantification of the relative protein expression (normalized to p38). The mean \pm Standard deviation (SD) of three independent experiments is shown. **E, F** Expression of JNK and p-JNK in ARPE-19 cells infected by AAV1-Rac1-GFP, -Q61L, or -T17N was examined by western blot analysis. Quantification of the relative protein expression (normalized to JNK). The mean \pm Standard deviation (SD) of three independent experiments is shown

A previous study revealed that coexpression of the RhoA dominant-negative inhibitory mutant RhoA-N19 suppressed PDGFR α expression [41], possibly because multiple Rho-responsive precursors are present on the PDGFR α promoter [42]. Rac1, a member of the Rho family, can significantly inhibit PDGFR β phosphorylation by suppressing the level of its GTP activity, but the precise mechanism of its regulation under the pathological conditions of PVR remains to be clarified.

We further explored potential cellular signaling regulatory mechanisms downstream of Rac1, which has been shown to be required for the activation of the downstream mitogen-activated protein kinase (MAPK)

signaling pathway in several inflammatory diseases and malignant tumors [26, 27, 43]. MAPK affects a wide range of cellular biological processes, including cell proliferation, differentiation, migration, survival, and stress responses [44], which mainly include the three classical branches of ERK, JNK, and p38 [45]. The MAPK signaling pathway has also been the subject of research in several ocular diseases [45, 46]. As such, we hypothesized that Rac1 may further regulate the pathological process of vitreous-stimulated PVR through the MAPK signaling pathway. As shown by our experimental results, phosphorylated ERK, p38, and JNK were differentially expressed upon vitreous stimulation, whereas GTP Rac1

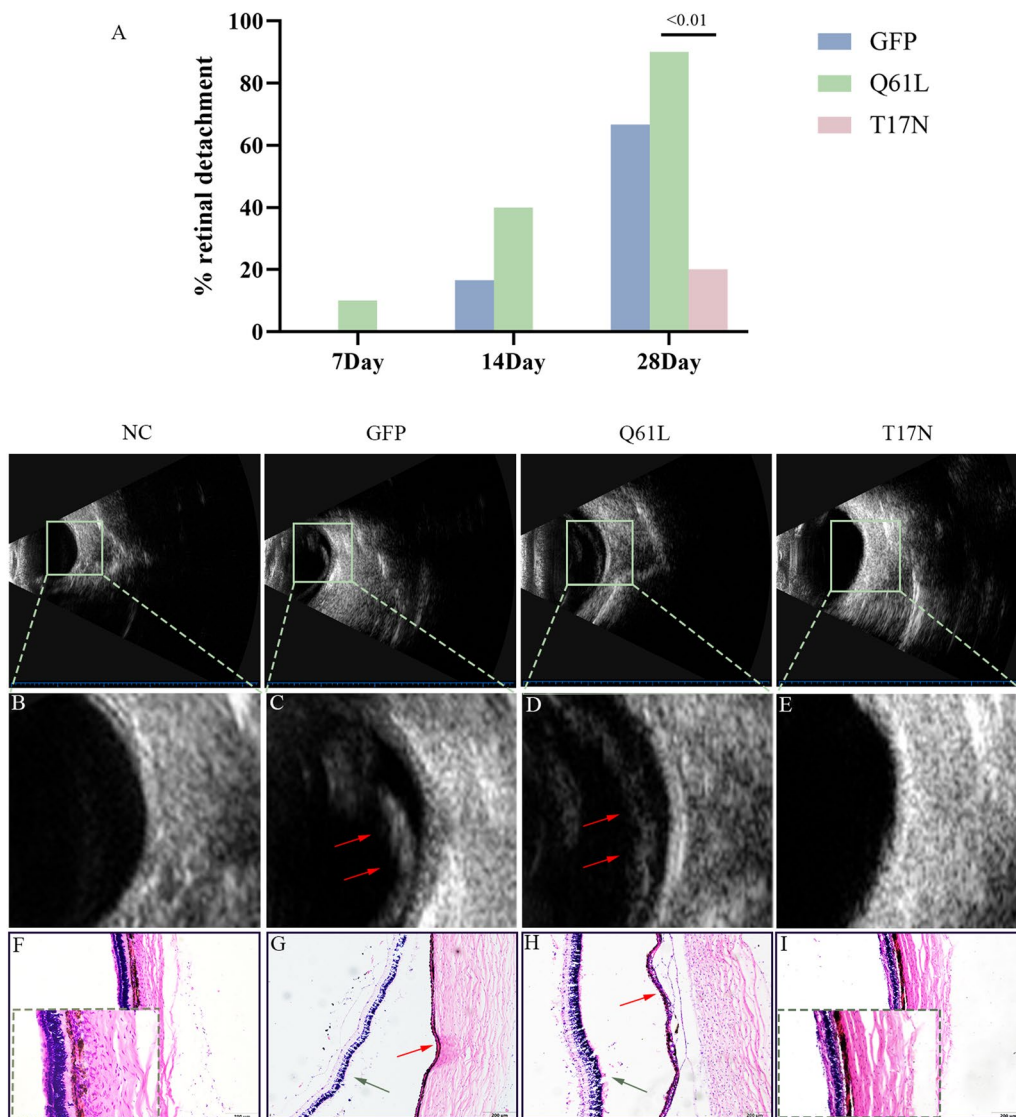


Fig. 7 Rac1T17N and Rac1Q61L attenuated and enhanced experimental PVR, respectively. **A** The percentage of rabbits with retinal detachment (stage 3 or higher) calculated for each time point. **B** Ultrasound detection in the control group. There was no significant abnormal echogenicity in the vitreous cavity. **C, D** In the rabbits injected with ARPE-19 cells transduced using AAV1-GFP (GFP) or AAV1-Rac1Q61L (Q61L), there were streak-like echoes and a band of echogenicity connected to part of the spherical wall. Red arrows pointing to striated echogenic bands indicate retinal detachment. **E** In the rabbits injected with ARPE-19 cells transduced using AAV1-Rac1T17N (T17N), there was no significant abnormal echogenicity. **F** Representative HE staining of the retina from the normal group. There was a clear structure of the whole layer of the normal rabbit retina. Normal structures of the retina from left to right: internal limiting membrane, nerve fiber layer, ganglion cell layer, inner plexiform layer, inner nuclear layer, outer plexiform layer, outer nuclear layer, external limiting membrane, photoreceptor layer, retinal pigment epithelium. **G** Representative HE staining of the retina from the GFP group. There was a complete detachment of the retinal neuroepithelium from the retinal pigment epithelium. The green arrow points to the retinal neuroepithelium and the red arrow points to the retinal pigment epithelium. **H** Representative HE staining of the retina from the Q61L group. There was complete detachment of the retinal pigment epithelium from the neuroepithelium and choroid. The green arrow points to the retinal neuroepithelium and the red arrow points to the retinal pigment epithelium. **I** Representative HE staining of the retina from the T17N group. There were clearer retinal structures and visible superficial retinal detachment. 10 \times

inhibition by transfection with T17N reversed these trends. These findings suggest that the pathological process of vitreous stimulation of PVR is regulated by the Rac1–MAPK signaling pathway.

PVR is a disease characterized by the presence of contractions upon the surface of the retina; these contractions eventually cause retinal detachment [22]. The experiments presented herein revealed that RPE cells

transduced with AAV1-Rac1T17N had less potential for proliferation, migration, invasion, and contraction. Importantly, in a rabbit PVR model generated via injection of PRP into the vitreous cavity, ARPE-19 cells transduced with AAV1-Rac1Q61L or Rac1T17N virus further demonstrated the role of Rac1 activity in PVR. The results revealed that retinal detachment was most severe after Rac1 activity was increased by the injection of ARPE-19 cells with Rac1Q61L, whereas PVR development was prevented in the group of injected ARPE-19 cells transduced with Rac1T17N. We assume that Rac1 enhances cell migration by regulating actin reorganization and that Rac1 activity is closely related to cell contractility, as the inhibition of Rac1 activity could weaken cell contractility and delay the development of PVR.

There may be some possible limitations in this study. Most researchers rely on the immortalized cell line ARPE19 for in vitro experimental studies due to its easy availability and culture, but owing to its abnormal karyotype and lack of several key features of differentiated RPE, ARPE19 no longer seems to be suitable for more in-depth studies as a natural RPE model [47]. Therefore, the selection of human primary retinal pigment epithelial cells or human stem cell-derived retinal pigment epithelial cells may provide a more reliable in vitro model for further study of the pathogenesis of PVR. In addition, PVR is a chronic disease and although we have improved the experimental details, there is still a gap between the cellular and animal models and the pathological process of human PVR, which needs to be further addressed in our future research. It is equally important to note that fundus photos can provide more convincing evidence for our experimental results, and it is therefore essential that we improve our techniques for presenting them in our research content in future studies.

Conclusions

In summary, our experimental results confirm that PDGFR β mediates vitreous-induced Rac1 activation in the ARPE-19 cells, as well as the important role of GTP Rac1 in regulating cellular responses intrinsic to PVR and PVR itself, indicating the potential of AAV1-Rac1T17N for PVR therapy.

Acknowledgements

Not applicable

Author contributions

DL, ML and JT performed the experiments, analyzed the data and wrote this manuscript; GY, CL and HY provided assistance on this study; HL, YH and XH designed the experimental program, acquired funding, and revised this manuscript. All authors read and approved the final manuscript.

Funding

This study was supported by grants from the National Science Foundation of China (81860172 and 82160199 to X.H.), Hainan Provincial Natural Science

Foundation of China (821RC1126 to X.H.), and Foreign Expert Project of Hainan Province (G20241024015E to H.L. and X.H.).

Availability of data and materials

The datasets used and/or analysed during the current study are available from the corresponding author on reasonable request.

Declarations

Ethics approval and consent to participate

This study was approved by the ethics committee of the First Affiliated Hospital of Hainan Medical University (2018–11).

Consent for publication

Not applicable.

Competing interests

The authors declare that they have no competing interests.

Author details

¹Department of Ophthalmology, The First Affiliated Hospital of Hainan Medical University, Haikou 570102, China. ²Key Laboratory of Emergency and Trauma of Ministry of Education, Department of Emergency Surgery, Key Laboratory of Hainan Trauma and Disaster Rescue, The First Affiliated Hospital, Hainan Medical University, Haikou 570102, China. ³Department of Ophthalmology, Shanghai General Hospital, Shanghai Jiao Tong University School of Medicine, Shanghai 200080, China.

Received: 22 October 2024 Accepted: 17 March 2025

Published online: 26 March 2025

References

- Pastor JC, Rojas J, Pastor-Idoate S, Di Lauro S, Gonzalez-Buendia L, Delgado-Tirado S. Proliferative vitreoretinopathy: a new concept of disease pathogenesis and practical consequences. *Prog Retin Eye Res.* 2016;51:125–55.
- Charteris DG. Proliferative vitreoretinopathy: revised concepts of pathogenesis and adjunctive treatment. *Eye.* 2020;34(2):241–5.
- Agrawal RN, He S, Spee C, Cui JZ, Ryan SJ, Hinton DR. In vivo models of proliferative vitreoretinopathy. *Nat Protoc.* 2007;2(1):67–77.
- Ma X, Xie Y, Gong Y, Hu C, Qiu K, Yang Y, et al. Silibinin prevents tgfb β -induced emt of rpe in proliferative vitreoretinopathy by inhibiting stat3 and smad3 phosphorylation. *Invest Ophthalmol Vis Sci.* 2023;64(13):47.
- Ma X, Han S, Liu Y, Chen Y, Li P, Liu X, et al. Dapl1 prevents epithelial-mesenchymal transition in the retinal pigment epithelium and experimental proliferative vitreoretinopathy. *Cell Death Dis.* 2023;14(2):158.
- Ferro Desideri L, Artemiev D, Zandi S, Zinkernagel M, Anguita R. Proliferative vitreoretinopathy: an update on the current and emerging treatment options. *Graefes Arch Clin Exp Ophthalmol.* 2024;262(3):679–87.
- Wang J, Zhao P, Chen Z, Wang H, Wang Y, Lin Q. Non-viral gene therapy using rna interference with pdgfr- α mediated epithelial-mesenchymal transformation for proliferative vitreoretinopathy. *Mater Today Bio.* 2023;20:100632.
- Yang Y, Huang X, Ma G, Cui J, Matsubara JA, Kazlauskas A, et al. Pdgfrb β plays an essential role in patient vitreous-stimulated contraction of retinal pigment epithelial cells from epiretinal membranes. *Exp Eye Res.* 2020;197:108116.
- Yang G, Huang Y, Li D, Tang J, Li W, Huang X. Silencing the long non-coding rna malat1 inhibits vitreous-induced epithelial-mesenchymal transition in rpe cells by regulating the pdgfrs / akt axis. *Int Ophthalmol.* 2024;44(1):363.
- Bianchi-Smiraglia A, Wolff DW, Marston DJ, Deng Z, Han Z, Moparthy S, et al. Regulation of local gtp availability controls rac1 activity and cell invasion. *Nat Commun.* 2021;12(1):6091.
- Bid HK, Roberts RD, Manchanda PK, Houghton PJ. Rac1: an emerging therapeutic option for targeting cancer angiogenesis and metastasis. *Mol Cancer Ther.* 2013;12(10):1925–34.

12. Davis MJ, Ha BH, Holman EC, Halaban R, Schlessinger J, Boggon TJ. Rac1 p29s is a spontaneously activating cancer-associated gtpase. *Proc Natl Acad Sci U S A*. 2013;110(3):912–7.
13. Liang J, Oyang L, Rao S, Han Y, Luo X, Yi P, et al. Rac1, a potential target for tumor therapy. *Front Oncol*. 2021;11:674426.
14. Majolee J, Podieh F, Hordijk PL, Kovacevic I. The interplay of rac1 activity, ubiquitination and gdi binding and its consequences for endothelial cell spreading. *PLoS ONE*. 2021;16(7):e0254386.
15. Cook DR, Rossman KL, Der CJ. Rho guanine nucleotide exchange factors: regulators of rho gtpase activity in development and disease. *Oncogene*. 2014;33(31):4021–35.
16. Huang X, Wei Y, Ma H, Zhang S. Vitreous-induced cytoskeletal rearrangements via the rac1 gtpase-dependent signaling pathway in human retinal pigment epithelial cells. *Biochem Biophys Res Commun*. 2012;419(2):395–400.
17. Huang XG, Chen YZ, Zhang ZT, Wei YT, Ma HZ, Zhang T, et al. Rac1 modulates the vitreous-induced plasticity of mesenchymal movement in retinal pigment epithelial cells. *Clin Exp Ophthalmol*. 2013;41(8):779–87.
18. Liu B, Burridge K. Vav2 activates rac1, cdc42, and rhoa downstream from growth factor receptors but not beta1 integrins. *Mol Cell Biol*. 2000;20(19):7160–9.
19. Sini P, Cannas A, Koleske A, Di Fiore P, Scita G. Abl-dependent tyrosine phosphorylation of sos-1 mediates growth-factor-induced rac activation. *Nat Cell Biol*. 2004;6(3):268–74.
20. Feng H, Li Y, Yin Y, Zhang W, Hou Y, Zhang L, et al. Protein kinase a-dependent phosphorylation of dock180 at serine residue 1250 is important for glioma growth and invasion stimulated by platelet derived-growth factor receptor α . *Neuro Oncol*. 2015;17(6):832–42.
21. Lei H, Qian CX, Lei J, Haddock LJ, Mukai S, Kazlauskas A. Rasgap promotes autophagy and thereby suppresses platelet-derived growth factor receptor-mediated signaling events, cellular responses, and pathology. *Mol Cell Biol*. 2015;35(10):1673–85.
22. Lei H, Rheaume MA, Velez G, Mukai S, Kazlauskas A. Expression of pdgfr α is a determinant of the pvr potential of arpe19 cells. *Invest Ophthalmol Vis Sci*. 2011;52(9):5016–21.
23. Fastenberg DM, Diddie KR, Dorey K, Ryan SJ. The role of cellular proliferation in an experimental model of massive periretinal proliferation. *Am J Ophthalmol*. 1982;93(5):565–72.
24. Li D, Huang Y, Lei H, Huang X. Dock1/elmo1/rac1 signaling is essential for vitreous-induced migration and contraction of arpe19 cells. *J Ocul Pharmacol Ther*. 2025. <https://doi.org/10.1089/jop.2024.0173>.
25. Zhou H, Cai L, Zhang X, Li A, Miao Y, Li Q, et al. Arhgef39 promotes tumor progression via activation of rac1/p38 mapk/atif2 signaling and predicts poor prognosis in non-small cell lung cancer patients. *Lab Invest*. 2018;98(5):670–81.
26. Jiang J, Zhang S, Shen H, Guan Y, Liu Q, Zhao W, et al. Rac1 signaling regulates cigarette smoke-induced inflammation in the lung via the erk1 / 2 mapk and stat3 pathways. *Biochim Biophys Acta Mol Basis Dis*. 2017;1863(7):1778–88.
27. Huang S, Deng W, Wang P, Yan Y, Xie C, Cao X, et al. Fermitin family member 2 promotes melanoma progression by enhancing the binding of p- α -pix to rac1 to activate the mapk pathway. *Oncogene*. 2021;40(37):5626–38.
28. Chiba C. The retinal pigment epithelium: an important player of retinal disorders and regeneration. *Exp Eye Res*. 2014;123:107–14.
29. Pastor JC, de la Rúa ER, Martin F. Proliferative vitreoretinopathy: risk factors and pathobiology. *Prog Retin Eye Res*. 2002;21(1):127–44.
30. Pennock S, Haddock LJ, Elliott D, Mukai S, Kazlauskas A. Is neutralizing vitreal growth factors a viable strategy to prevent proliferative vitreoretinopathy? *Prog Retin Eye Res*. 2014;40:16–34.
31. Zhu Z, Yu Z, Rong Z, Luo Z, Zhang J, Qiu Z, et al. The novel gins4 axis promotes gastric cancer growth and progression by activating rac1 and cdc42. *Theranostics*. 2019;9(26):8294–311.
32. Xia L, Lin J, Su J, Oyang L, Wang H, Tan S, et al. Diallyl disulfide inhibits colon cancer metastasis by suppressing rac1-mediated epithelial-mesenchymal transition. *Onco Targets Ther*. 2019;12:5713–28.
33. Sauzeau V, Beignet J, Bailly C. Rac1 as a target to treat dysfunctions and cancer of the bladder. *Biomedicines*. 2022;10(6):1357.
34. Acuner SE, Sumbul F, Torun H, Haliloglu T. Oncogenic mutations on rac1 affect global intrinsic dynamics underlying gtp and pak1 binding. *Biophys J*. 2021;120(5):866–76.
35. Zhang P, Zhang X, Fan J, Hao X, Wang Y, Hui Y, et al. Rac1 activates hif-1 in laser induced choroidal neovascularization. *Int J Ophthalmol*. 2011;4(1):14–8.
36. Zhang M, Zhao G, Hou Y, Zhong S, Xu L, Li F, et al. Rac1 conditional deletion attenuates retinal ganglion cell apoptosis by accelerating autophagic flux in a mouse model of chronic ocular hypertension. *Cell Death Dis*. 2020;11(9):734.
37. Kotterman MA, Schaffer DV. Engineering adeno-associated viruses for clinical gene therapy. *Nat Rev Genet*. 2014;15(7):445–51.
38. Xu X, Chen W, Zhu W, Chen J, Ma B, Ding J, et al. Adeno-associated virus (aav)-based gene therapy for glioblastoma. *Cancer Cell Int*. 2021;21(1):76.
39. Zhang H, Zhan Q, Huang B, Wang Y, Wang X. Aav-mediated gene therapy: advancing cardiovascular disease treatment. *Front Cardiovasc Med*. 2022;9:952755.
40. Gilger BC, Hirsch ML. Therapeutic applications of adeno-associated virus (aav) gene transfer of hla-g in the eye. *Int J Mol Sci*. 2022;23(7):3465.
41. Kumar R, Ha J, Radhakrishnan R, Dhanasekaran D. Transactivation of platelet-derived growth factor receptor α by the gtpase-deficient activated mutant of galpha12. *Mol Cell Biol*. 2006;26(1):50–62.
42. Kawagishi J, Kumabe T, Yoshimoto T, Yamamoto T. Structure, organization, and transcription units of the human α -platelet-derived growth factor receptor gene, PDGFRA. *Genomics*. 1995;30(2):224–32.
43. Datta C, Das P, Swaroop S, Bhattacharjee A. Rac1 plays a crucial role in mcp-1-induced monocyte adhesion and migration. *Cell Immunol*. 2024;401:104843.
44. Yan Y, Dai T, Guo M, Zhao X, Chen C, Zhou Y, et al. A review of non-classical mapk family member, mapk4: a pivotal player in cancer development and therapeutic intervention. *Int J Biol Macromol*. 2024;271(Pt 2):132686.
45. Moustardas P, Aberdam D, Lagali N. Mapk pathways in ocular pathophysiology: potential therapeutic drugs and challenges. *Cells*. 2023;12(4):617.
46. Muraleva NA, Kolosova NG. P38 mapk signaling in the retina: effects of aging and age-related macular degeneration. *Int J Mol Sci*. 2023;24(14):11586.
47. Datlibagi A, Zein-El-Din A, Frohly M, Willermain F, Delporte C, Motulsky E. Experimental models to study epithelial-mesenchymal transition in proliferative vitreoretinopathy. *Int J Mol Sci*. 2023;24(5):4509.

Publisher's Note

Springer Nature remains neutral with regard to jurisdictional claims in published maps and institutional affiliations.